Available online at www.sciencedirect.com
ScienceDirect
Carbohydrate Polymers 72 (2008) 625–637
Carbohydrate Polymers
www.elsevier.com/locate/carbpol

Modeling of α(1–4) chain arrangements in α(1–4)(1–6) glucans: The action and outcome of β-amylase and *Pseudomonas stutzeri* amylase on an α(1–4)(1–6) glucan model

N.K. Matheson, R.A. Caldwell *

Faculty of Agriculture, Food and Natural Resources, The University of Sydney, Sydney, NSW 2006, Australia

Received 3 August 2007; received in revised form 27 September 2007; accepted 4 October 2007
Available online 12 October 2007

This publication is dedicated to Norman K. Matheson who passed away on the 15th July, 2007 soon after the final draft was completed.

Abstract

Simulated enzymic debranching of a β-limit dextrin model, prepared from a computed construct made by random extension and branching, and given the CCL value of *w*-maize amylopectin (and equal amounts of external chains with ECL values of 2 and 3) has been related to experimental chromatograms of the debranched β-limit dextrin of the amylopectin. The profile was similar to those from gel chromatograms and IEC-PAD chromatography.

The equivalent lengths in glucosyl units of grid-links (g-links) of internal and external chains in constructs were calculated from the ICL and ECL values of amylopectin and models produced from the constructs with the appropriate lengths for internal and external chains. These derived models were subjected to simulated hydrolysis by *Pseudomonas stutzeri* amylase and the products compared with those of the experimental distribution from *w*-maize amylopectin. With the model the amounts of maltotetraose and maltodextrins released were similar to the experimental values but the distribution of branched maltodextrins was quite different. Unlike *w*-maize amylopectin – a polymer with the cluster structure – which has given a profile of molecular sizes of maltodextrins with low amounts of single and small numbers of internal chains and with a peak at a M_W of about 14,000 (13 chains), in the model the proportion of maltodextrin with one internal chain was high and as d.p. increased the amounts decreased exponentially. This would be expected if the distribution of internal chains in the core was random. It is suggested that in the core of a model prepared from a construct made with alternating probabilities of extension – one in which this probability is high relative to branching, and a second in which it is low – may give clusters of branched maltodextrins with short internal chains which are joined by longer chains; more closely approximating the distribution of internal chains of different lengths in amylopectin.

An arrangement for amylopectin molecules in the starch granule has been proposed. In this, they have a wafer-like, discoidal shape, composed of the amorphous zone overlain with the double helical, crystalline region. The flat macromolecules are concentrically layered with the former on the inside and the latter oriented to the outside of the granule.

Keywords: Amylopectin; Glycogen; α(1–4) Glucan; β-Limit dextrin

1. Introduction

For the development of a model describing the proportions of α(1–4) chains with different lengths and levels of branching and possible arrangements of these in amylopectin, dendrimeric constructs have been generated by programs involving random selection for extension and branching of chains (Matheson & Caldwell, 1999). Initially construction was made without any spatial restrictions (R-SU constructs). This led to a convergent series of the proportion of longer B chains with an increasing degree of branching. The ratio of probabilities of extension and branching determines the proportions of the different types of chains (A and B_k). In a subsequent study constructs in two and three dimensional space were generated (Caldwell

* Corresponding author. Tel.: +61 2 9351 2815; fax: +61 2 9351 5108.
E-mail address: r.caldwell@usyd.edu.au (R.A. Caldwell).

0144-8617/$ - see front matter
doi:10.1016/j.carbpol.2007.10.006

& Matheson, 2003). The introduction of steric restriction reduces the proportions of B chains with medium levels of branching and increases both those with one branch and with high k values. Models with appropriate values of average chain lengths (CL, ICL, ECL, and CCL) for particular amylopectins were then prepared from the constructs. From comparison of the numbers of chains of each d.p. with chromatograms of debranched amylopectin, the chain length distribution of spatially restricted models was found to have a general resemblance to amylopectin. Abbreviations used previously appear in Caldwell and Matheson (2003); Matheson and Caldwell (1999). New abbreviations are given in Table 1 or explained where they appear in the text.

As well as complete debranching at α(1–6) linkages, several other enzymic procedures indicating aspects of the distribution of α(1–4) chains have been performed. Amylopectins have been partly depolymerised with amylases. The *exo*-amylase, β-amylase, shortens both A chains and the outermost sections of B chains. The resultant β-limit dextrins have been debranched and the α(1–4) chains examined chromatographically (Baba & Arai, 1984; Inouchi, Glover, & Fuwa, 1987; Klucinec & Thompson, 2002; Mercier, 1973; Shi & Seib, 1995; Yuan, Thompson, & Boyer, 1993). The *endo*-amylase from *Bacillus subtilis (amyloliquefaciens)* (Priest, Goodfellow, Shute, & Berkeley, 1987) requires long sections of α(1–4) chains for rapid hydrolysis (Robyt & French, 1963) and the chromatographic behaviour of the products also gives information about the clusters (Bertoft & Koch, 2000; Bertoft & Spoof, 1989; Bertoft, Zhu, Andtfolk, & Jungner, 1999).

The amylase from *P. stutzeri* (Finch & Sebesta, 1992; Nakakuki, Azuma, & Kainuma, 1984; Schmidt & John, 1979) rapidly *exo*-hydrolyses external chains, producing maltotetraose, and then, much less rapidly *endo*-hydrolyses longer internal chains, giving more maltotetraose and branched maltodextrins that indicate the nature and arrangement of clusters.

The aim of this work is to model the action and outcome of firstly, β-amylolysis and secondly, *P. stutzeri* amylolysis on a computed construct of *w*-maize amylopectin.

2. Methods

2.1. Construct generation and fragmentation

Constructs were generated according to the spatially restricted algorithm given in a previous publication (Caldwell & Matheson, 2003). The construct is comprised of monomeric units henceforth referred to as *g-links*. Comparison of the characteristics of the construct with that of an amylopectin molecule (Caldwell & Matheson, 2003) provides a means of equating a g-link to a number of glucosyl units. This number varies slightly depending on whether the g-link is in an external A or B, or internal B chain. Simulated β-amylolysis is achieved by removal of g-links from the external A and B chains of the construct.

Fragmentation (or simulated hydrolytic cleavage) by *P. stutzeri* amylase and the tabulation of the resultant fragment sizes is achieved by a sequential reversal of the construction algorithm with a restriction on the minimum number of g-links between branch points that can undergo cleavage. When hydrolysis occurs the glucosyl units of the middle part of an internal chain are released as maltotetraosyl units and the g-links at the ends become modified stubs attached to the two released branched units. This is illustrated in Fig. 1. These are cleavage diagrams when the minimum number of hydrolysable, internal unbranched g-links is 2 as in *w*-maize amylopectin. In the simulated hydrolysis of mammalian glycogen this number is 3. The action of *P. stutzeri* amylase was chosen because of its specific release of only maltotetraose from internal B chains.

Table 1
Formulae for the calculation of mean numbers of g-links in chains and segments of constructs

Chain type	Symbol for average length		Calculation of L values
	In α(1–4)(1–6) glucans (glucosyl units)	In constructs (g-link units)	
A	CL_A[a]	L_A	[b]
B Segments	$CL_B/(F+1)$[a]	L_{BS}	[b]
External B	ECL_B[a]	L_{EB}	[b]
External (A + B)	ECL	L_E	$=aL_A + bL_{EB}$
B	CL_B	L_{BC}	$=(F+1)L_{BS} = F * L_I + L_{EB}$
Whole	CL	L_C	$=aL_A + bL_{BC} = aL_A + b(F+1)L_{BS}$
All segments	$CL_S \approx CL/2$	L_S[c]	$=0.5aL_A + 0.5bL_{EB} + 0.5L_I$ $=0.5aL_A + 0.5(b+1)L_{BS}$
Internal	ICL + 1	L_I	$=2L_S - aL_A - bL_{EB}$ $=(b+1)L_{BS} + aL_A - aL_A - bL_{EB}$ $=(b+1)L_{BS} - bL_{EB}$
Core	CCL + 1	L_{CC}	$=F * L_I$

[a] Cannot at present be measured.
[b] From output of program.
[c] The total number of segments (A plus B chains and internal segments including one branch point) is $2T - 1$: the numbers of A chains, external B and internal segments are aT, bT and T, respectively (for a large number of chains).

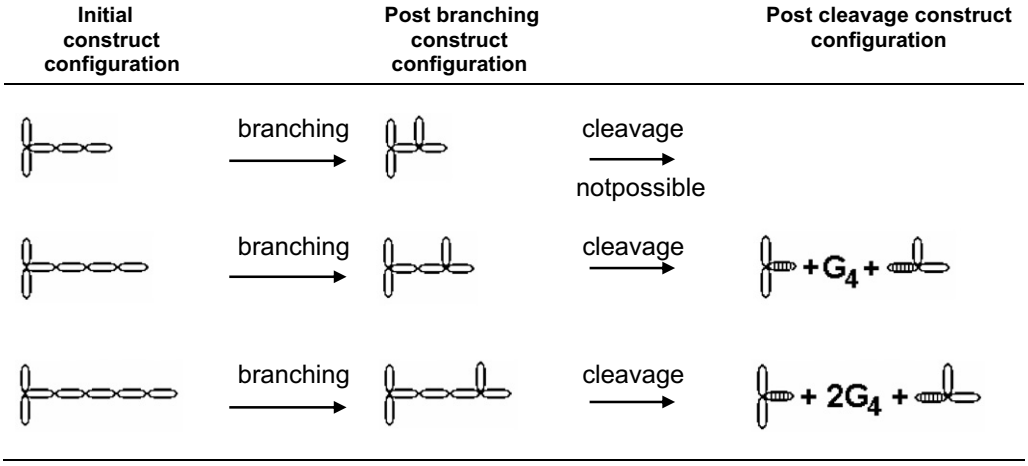

Fig. 1. An example of the cleavage of internal construct linkages when the minimum number of internal, unbranched g-links required for cleavage is 2. A maltotetraosyl unit is represented as $\mathbf{G}_4$. The symbol represents a modified g-link.

3. Results and discussion

3.1. Comparison of the structure of the β-limit dextrin of w-maize amylopectin with that of a model prepared from a construct

β-Amylolysis of amylopectin gives a limit dextrin containing shortened A chains of two or three glucosyl units. A number of studies by SEC of the α(1–4) chain profile of the debranched β-limit dextrin of *w*-maize amylopectin have been reported (Baba & Arai, 1984; Inouchi et al., 1987; Klucinec & Thompson, 2002; Yuan et al., 1993); and also by IEC-PAD (Shi & Seib, 1995) and HPAEC-PAD (Bertoft, 2004).

The construct used was the spatially restricted one (3D(R)($Z = 3$)) that gave the debranching profile shown in Fig. 5A in Caldwell and Matheson (2003) (henceforth referred to as the 3D(R) construct). The types and numbers of chains from this construct were A(693), B_1(310), B_2(116), B_3(45), B_4(30), B_5(21), B_6(12), B_7(10), B_8(6), B_9(5), B_{10}(2), B_{11}(2), B_{12}(2), B_{13}(1), B_{14}(1), B_{15}(1). β-Limit dextrins have equal numbers of A chain stubs of two or three glucosyl units whilst the mean DP of a B chain with k branches is k(ICL + 1) + 1.5. The ICL was taken as similar to that of *w*-maize amylopectin (Yun & Matheson, 1993). Fig. 2 shows the amounts of glucan vs. d.p. for the α(1–4) chains of the β-limit dextrin of the model. The B chain numbers were convolved assuming a series of normal distributions each with a standard deviation of 3.5. The amounts of A chains have been taken as one half of each of two and three glucosyl units. The peak value (as weight of glucan) occurs at d.p. 10–11. In a comparison of the relative weights of glucan for the model with an IEC-PAD plot of debranched *w*-maize β-limit dextrin (Shi & Seib, 1995) both had peaks at closely similar values, 9–10 and 10–11. However, two differences were apparent. In the chromatographic plot the weights at d.p. 4–7 were much higher, and those from d.p. 14 to 18 lower, although overall the two curves had a relatively similar shape. The experimental chromatogram was published before the introduction of post-column depolymerisation prior to estimation by PAD (Wong & Jane, 1997). In this method of assay, in the absence of depolymerisation, the detector response decreases as the d.p. increases. Also, when *w*-barley β-limit dextrin was debranched with isoamylase and chromatographed on Biogel P-4 (Fig. 5c and d in MacGregor & Morgan, 1984) and *w*-rice β-limit dextrin debranched with pullulanase and chromatographed on Biogel P-2 (Fig. 1 in Enevoldson & Juliano, 1988) very small peaks due to maltotetraose were obtained. Estimation in both was with orcinol-H_2SO_4. This oligosaccharide derives from B_1 chains with an ICL of 1 or 2. The weight of glucan in chains of d.p. 4 and 5 in the IEC-PAD plot of debranched *w*-maize β-limit dextrin implies that the number of B_1 chains with an ICL of 1 or 2 in the β-limit dextrin is about twice that of chains at the peak values of d.p. 9 and 10. Conversion of the amounts of glucan in α(1–4) chains of d.p.4–48 in the IEC-PAD plot to numbers of chains leads to a CL of 11, giving a CCL of 9.5. The CCL for the model in the same range of d.p. was 13. *w* maize amylopectin (and hence its β-limit dextrin) as well as the model to a d.p. 126 have a CCL of 14.

In another examination of debranched *w*-maize and potato β-limit dextrin by IEC-PAD, (Fig. 4 in Bertoft, 2004) large responses were found for short chains (up to 9). Estimation of the A chain content of *w*-maize β-limit dextrin, calculated as

$$\frac{0.5 * \text{detector response of d.p.} = 2 + 0.33 * \text{detector response of d.p.} = 3}{\sum_{i=2}^{i=44} \frac{\text{detector response of d.p.} = i}{i}}$$

gave a value of 0.75 (an A to B chain ratio ≈3:1) but β-amylolysis of amylopectin does not alter the *a* value, which for *w*-maize is 0.55. Also, the ratio of number of chains of d.p. 2 to those of d.p. 3, equal to

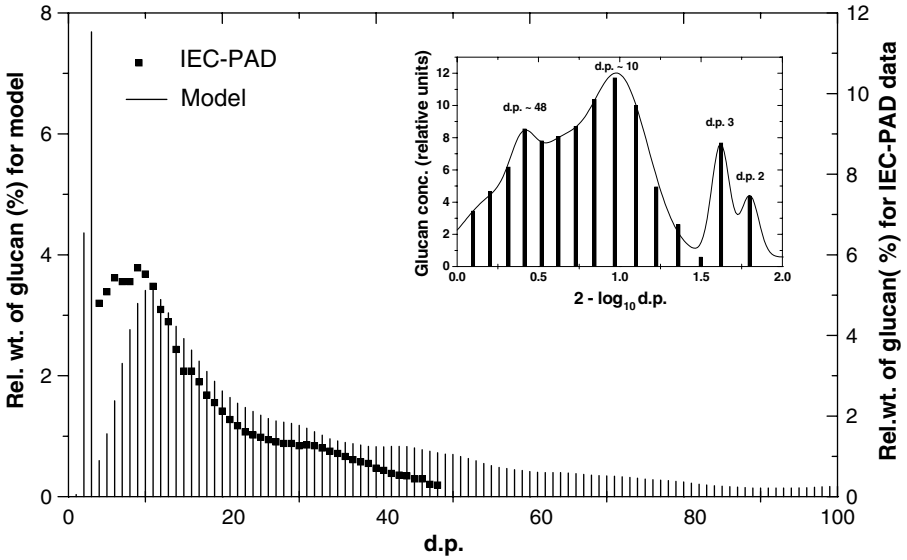

Fig. 2. A comparison of the glucan mass distribution vs d.p. for the model and the data of Shi and Seib (1995) for debranched *w*-maize amylopectin. The inset is a transform of the model data from a d.p. scale to a log d.p. scale.

$\frac{0.5 * \text{detector response of d.p.} = 2}{0.33 * \text{detector response of d.p.} = 3}$ is 1.6, whereas it should be 1.

Since the plots being compared in Fig. 2 are relative percentages, reduction of the amounts of chains of d.p. 4–7 would raise the values at the higher d.p. values. This combined with higher values for longer chains – when estimated after depolymerisation – could be expected to lead to a graph of the experimental chromatogram closer to the model. The results indicate that a construct, prepared by random extension and branching and given the CL, ECL and CCL values of *w*-maize amylopectin β-limit dextrin, when subjected to simulated debranching gives a distribution of α(1–4) chains similar to experimental values.

Debranched chains in the model are plotted as the concentration of glucan in B chains vs. log d.p. and shown in the inset in Fig. 2. Precise comparison of simulated debranching of the model and experimental SEC of debranched *w*-maize β-limit dextrin is not possible, since in SEC a nearly linear relationship between elution volume and log d.p. is not maintained towards the ends of the inclusion range of the matrix (Andrews, 1965). Also, all material larger than the maximum size for inclusion elutes at the exclusion volume. However, SEC of *w*-maize β-limit dextrin (Fig. 2 in Yuan et al., 1993; Fig. 1 in Klucinec & Thompson, 2002) and also *w*-rice (Fig. 5 in Inouchi et al., 1987) and *w*-barley (Fig. 4 in MacGregor & Morgan, 1984) β-limit dextrins indicated ranges of debranched B chains up to about d.p. 100, similar to that of the model. As well within this range they consisted of two major, broad peaks – one in the region of d.p. 10 and the other near 40. In the model of *w*-maize β-limit dextrin, B_1 chains have peaks at DP 10–12 and B_6 chains at 45–48.

3.2. Estimation of the average number of glucosyl units in a g-link for the A, internal B and external B chains of a construct corresponding to a specific amylopectin or glycogen model

Three types of structure have had aspects of their chain distribution compared. The first is the computed construct, in which chains are composed of g-links, and have a characteristic distribution of B chain lengths with different degrees of branching and numbers and disposition of internal chains of differing average chain lengths. With spatial restriction [3D(R) or 3D(P)] the number of B_1 chains is higher, of B_{2-5} chains lower, and of chains with more than five branches higher than the R-SU values (Caldwell & Matheson, 2003).The second structure is the model prepared from the 3D(R) construct by setting ECL and ICL values (in glucosyl units) equal to those of a natural amylopectin. The third structure is the natural amylopectin with its *a* value, average chain lengths and characteristic structure. The chromatographic profile of the α(1–4) chains produced by debranching the last provides the experimental data for the α(1–4) chain distribution.

In computed constructs the mean length of each type of chain comes from a distribution of numbers of g-links. In models of amylopectin (and glycogen) the average chain lengths (internal and external) are in glucosyl units. In comparing the behavior of models derived from computed constructs with amylopectin (or glycogen) to decide the likelihood of amylolytic hydrolysis of an internal or external chain, it is necessary to estimate the average number of glucosyl units represented by a g-link unit for each type of chain.

The 3D(R) construct for amylopectin gave on debranching the profile of weight of glucan vs d.p. of α(1–4)

chains shown in Fig. 5A in Caldwell and Matheson, 2003 and labeled 3D(R)($Z = 3$). From the computed outputs of mean numbers of g-links in external A (L_A), external B (L_{EB}) and segments of B chains (L_{BS}), means for external (L_E) and internal (L_I) chains, as well as average lengths of B (L_{BC}), whole (L_C), and core (L_{CC}) chains and also average segment lengths of whole chains (L_S), can be derived (Table 1). Then, for a particular α(1–4)(1–6) glucan, the average number of glucosyl units represented by one g-link in external and internal chains in the construct can be estimated. For an external chain it is ECL/L_E and hence for a chain composed of n g-links the length (in glucosyl units) is $n * (\mathrm{ECL}/L_E)$. For internal chains one g-link represents $[(\mathrm{CCL}+1)/L_{CC}]$ glucosyl units. Table 2 shows the mean lengths (in g-links) of the various types of chains in the described construct ($a = 0.55$), and also the average chain lengths (in glucosyl units) in the chains of three genotypes of maize (*w*, *n* and *ae*). In internal chains the g-link at one end includes a section that is a branch point and corresponds to one glucosyl unit, so an internal chain composed of n g-links consists of $n * [(\mathrm{CCL}+1)/L_E] - 1$ glucosyl units. The last two lines give estimates of the average number of glucosyl units in a g-link unit of external and internal chains for each type of amylopectin. Table 3 does the same for a construct of mammalian glycogen.

Table 3
Mean chain lengths (in g-links) of a computer construct [3D(R)], $E_A = 0.80$, $E_B = 0.20$, $B_A = 2$, $B_B = 2$, X,Y and $Z = 60$ g-links, $a = 0.42$] and the equivalent average chain lengths (in glucosyl units) in mammalian glycogen[a]: the number of glucosyl units in one g-link of external and internal chains of the model derived from this construct

Construct		Glycogen	
Chain length symbol	Value (g-links)	Chain length symbol	Value (glucosyl units)
L_A	1.51	–	–
L_{BS}	1.47	–	–
L_{EB}	1.57	–	–
L_E	1.55	ECL	8
L_{BC}	3.89	–	–
L_C	2.86	CL	14
L_S	1.43	CL_S	7
L_I	1.32	ICL + 1	6
L_{CC}	2.32	CCL + 1	11
		ECL/L_E	5.2
		(CCL + 1)/L_{CC}	4.7

[a] Chain length data from Yun and Matheson (1993).

3.3. Determination of the distribution of internal chains of varying lengths in the core chains of models fitted to constructs prepared by random extension and branching

From a wide range of physico-chemical evidence and examination of the partial hydrolysis products of amylopectin, the accepted formula is the cluster structure (French, 1984; Kainuma, 1988; Manners, 1989; Zobel, 1988). In this structure, core chains have α(1–6) branches. The sections between adjacent branches are internal chains of varying lengths. In the cluster structure branched maltodextrins with short internal chains are joined by longer unbranched chains. The short internal chains are not hydrolysed (or very slowly) by *endo*-amylases, whereas the longer unbranched chains linking the maltodextrin clusters are hydrolysed more rapidly. For amylopectin the models that have been proposed can be broadly divided into two types: those in which the A and external B chains (the outermost section of a B chain) are depicted with varying chain lengths (Hizukuri, 1986; Manners & Matheson, 1981; Robin, Mercier, Duprat, Charbonniere, & Guilbot, 1975) or those with these chains having a more constant length (Bertoft, 2004; Gallant, Bouchet, & Baldwin, 1997; Imberty, Buleon, Tran, & Perez, 1991 Jenkins, Cameron, & Donald, 1993; Nikuni, 1978; Oostergetel & van Bruggen, 1993; Waigh et al., 2000; Yamaguchi, Kainuma, & French, 1979). The former are usually proposed from studies on solubilised amylopectin – and are formulae showing pri-

Table 2
Mean chain lengths (in g-links) of a computer construct [3D(R)], $E_A = 0.60$, $E_B = 0.40$, $B_A = 2$, $B_B = 2$, X and $Y = 60$ and $Z = 3$ g-links, $a = 0.55$] and the equivalent average chain lengths (in glucosyl units) in amylopectins from three genotypes of maize[a]: the number of glucosyl units in one g-link of external and internal chains of the models derived from this construct

Construct		Amylopectin			
Chain length symbol	Value (g-links)	Chain length symbol	Value (glucosyl units)		
			w	*n*	*ae*
L_A	1.62	–	–	–	–
L_{BS}	1.43	–	–	–	–
L_{EB}	1.80	–	–	–	–
L_E	1.70	ECL	12	14	17
L_{BC}	4.57	–	–	–	–
L_C	2.96	CL	18	22	33
L_S	1.48	CL_S	9	11	17
L_I	1.27	ICL + 1	7	8	11
L_{CC}	2.78	CCL + 1	15	18	26
		ECL/L_E	7.1	8.2	10.0
		(CCL + 1)/L_{CC}	5.4	6.5	9.4

[a] Chain length data from Yun and Matheson (1993).

mary structure without consideration of conformational effects – whereas the latter are associated with physicochemical measurements on granules or amorphous, solid-state material, and include the representation of double helical regions. The conformation adopted in solution is unlikely to be the same as that in the solid state (Gidley & Bociek, 1985). Solution studies indicate a range of α(1–4) chain lengths: complete debranching gives smooth chromatographic profiles of α(1–4) chains on PAD-IEC (Jane et al., 1999).

In a number of models – usually two-dimensional representations – the clusters are shown to be of relatively uniform size and appearance, and in a regular pattern (Jenkins et al., 1993; Kainuma, 1988; Nikuni, 1978; Yamaguchi et al., 1979). In others they are shown as differing in size and shape and not arranged regularly (Hizukuri, 1986; Manners, 1989; Manners & Matheson, 1981; Robin et al., 1975).

Partial hydrolysis with enzymes or acid gives α(1–6) branched maltodextrins of a range of sizes (Bertoft & Spoof, 1989; Finch & Sebesta, 1992). X-ray crystallography of granules shows the presence of ordered structures in which some α(1–4) chains are involved in parallel double helices (Imberty et al., 1991). The extended nature of the chains in this double helix is shown by a comparison of the advance along the helical axis due to the addition of one glucosyl residue ($h = 0.35$) with the value for V amylose ($h = 0.13$) and the distance between O_1 and O_4 in the α-glucosyl structure (0.45 nm).These crystalline regions are considered to involve double helical formation between an outermost segment of B chains and an A chain attached as the outermost branch. (CP/MAS) ^{13}C NMR spectroscopy has shown the presence of both crystalline and amorphous regions in granules and re-precipitated amylopectin (Cooke & Gidley, 1992; Gidley & Bociek, 1985). Electron microscopy also shows regions of organization within granules (Gallant et al., 1997; Nikuni, 1978; Yamaguchi et al., 1979).

A further structural aspect of amylopectin is the distribution of internal chains with differing lengths that produce the clusters. The amylase from *P. stutzeri* rapidly releases maltotetraose units from the external chains of amylopectin, and then more slowly hydrolyses some internal chains (Finch & Sebesta, 1992; Nakakuki et al., 1984; Robyt & Ackerman, 1971; Schmidt & John, 1979). Hydrolysis of unbranched α(1–4) chains starts at the non-reducing end, removing tetrasaccharide units sequentially.

SEC of the products from reaction of wheat amylopectin with *P. stutzeri* amylase – reacted until the reducing power of the mixture was constant – gave a peak due to maltotetraose as well as a broad peak with a maximum at an elution volume corresponding to that of a dextran with a M_W of about 14,000 (Finch & Sebesta, 1992). The range of M_S values was broad; from maltotetraose to that of a dextran standard of 250,000. All of the original polysaccharide had been partly depolymerised. Precipitation from the solution with ethanol, followed by a second amylase treatment of the re-dissolved precipitate and ethanol precipitation gave material that on SEC had a peak at the elution volume of dextran with a M_W of 12,000 and a range of 70,000 down to that of maltotetraose, The wide range of the fraction of branched α(1–4)(1–6) dextrins indicated considerable variation in the structures of these and hence in those of the clusters. NMR indicated an average M_W of 14,300.

In estimating the extent of simulated hydrolysis of external chains in models, the number of units was assigned as the number of whole tetramer units that could be released after subtraction of a stub of three glucosyl units. Table 4 shows the estimated average numbers of glucosyl units in external chains with varying numbers of g-links of a model of *w*-maize amylopectin prepared from the 3D(R) construct and the calculated numbers of maltotetraose units released from these external chains of different lengths. In external chains a g-link represents more glucosyl units than in internal chains. In this construct the fraction of g-links in core chains is 0.43, whereas in *w*-maize amylopectin the fraction of glucan is 0.34 (Matheson, 1995).

The partial hydrolysis of blue starch (Nakakuki et al., 1984; Schmidt & John, 1979) and of the β-limit dextrin of amylopectin shows that the enzyme can also hydrolyse by an *endo* mechanism. Although *P. stutzeri* amylase can hydrolyse an α(1–4) linkage in the glucosyl unit next to the unit linked α(1–6) in the maltotetraosyl sections of

Table 4A
Average numbers of glucosyl units in models of *w*-maize amylopectin corresponding to chains of different numbers of g-links in the constructs, numbers of maltotetraosyl units released on hydrolysis and numbers of glucosyl units in remnant internal and external segments

No. of g-links		1	2	3	4	5	6	7	8
External chains ECL/$L_E = 7.1$	Average No. of glucosyl units[a]	7	14	21	28	36	43	50	57
	No. of G_4 units released[b]	1	2	4	6	8	9	11	13
	Glucosyl units remaining[c]	3.1	6.2	5.3	4.4	3.5	6.6	5.7	4.8
Internal chains (CCL + 1)/$L_{CC} = 5.4$	Average No. of glucosyl units[a]	4	10	15	21	26	31	37	42
	No. of G_4 units released[b]	0	1	2	3	5	6	7	9
	Glucosyl units remaining[c]	–	5.8	7.2	8.6	6.0	7.4	8.8	6.2

[a] To the nearest whole number.
[b] Whole number part of calculated value.
[c] Shared between two remnant external segments.

Table 4B
Average numbers of glucosyl units in models of mammalian glycogen corresponding to chains of different numbers of g-links in the construct, numbers of maltotetraosyl units released on hydrolysis and numbers of glucosyl units in remnant external and internal segments

No. of g-links		1	2	3	4	5	6	7	8
External chains ECL/$L_E = 5.2$	Average No. of glucosyl units[a]	5	10	16	21	26	31	36	42
	No. of G_4 units released[b]	0	1	3	4	5	7	8	9
	Glucosyl units remaining[c]	–	6.4	3.6	4.8	6.0	3.2	4.4	5.0
Internal chains (CCL + 1)/$L_{CC} = 4.8$	Average No. of glucosyl units[a]	4	9	13	18	23	28	33	37
	No. of G_4 units released[b]	0	0	1	3	4	5	6	7
	Glucosyl units remaining[c]	–	–	9.4	6.2	7.8	7.8	8.6	9.4

[a] To the nearest whole number.
[b] Whole number part of calculated value.
[c] Shared between two remnant external segments.

pullulan, the limited extent of the hydrolysis of the β-limit dextrin of wheat amylopectin (11%) indicates that where α(1–4) chains have α(1–6) branch points at both ends that hydrolysis is much more restricted. With wheat amylopectin β-limit dextrin the branched dextrin fraction left after hydrolysis had an average chain length of 6.4 and an estimated average d.p. of 47.

In simulated hydrolysis of the models, the number of maltotetraosyl units released from an internal chain was assigned as the number of whole tetramer units remaining after subtraction of $2 * 3$ glucosaccharide units from the ICL: two stubs of at least three glucosyl units remain at the two branch points. Table 4A shows the estimated average numbers of glucosyl units in the internal chains of models of *w*-maize amylopectin consisting of different numbers of g-links and derived from 25 replicates of the 3D(R) construct $E_A = 0.60$, $E_B = 0.40$, $B_A = 2$, $B_B = 2$, X, $Y = 60$, $Z = 3$, $T = 1000$, total g-links = 2964. The calculated numbers of maltotetraosyl units released have also been estimated. For external chains it equals

$$\frac{\left[\left(\frac{\mathrm{ECL}}{L_E}\right) * (\text{no. of g-links}) - 3\right]}{4}$$

whilst for internal chains:

$$\left[\frac{\mathrm{CCL}+1}{L_{CC}}\right] * \frac{[(\text{no. of g-links} - 1) - (2 * 3)]}{4}$$

with the whole number part of the answer giving the number of maltotetraosyl units released.

This means that in the construct corresponding to the *w*-maize amylopectin model all external chains lose maltotetraosyl units – to varying degrees – according to the number of g-links they consist of, and that internal chains made up of one g-link are not hydrolysed, whereas all others react, releasing varying numbers of maltotetraosyl units according to their composition of g-links (Table 4A).

With the construct corresponding to the mammalian glycogen model, external chains of one g-link are not hydrolysed and internal chains need to be composed of at least three g-links for hydrolysis and release of maltotetraosyl units to occur (Table 4B).

The branched maltodextrins produced by hydrolysis of α(1–4)(1–6) glucans by *P. stutzeri* amylase consist of:

(i) Contiguous short internal chains that have not been hydrolysed.
(ii) Remnant external chains that result from *exo*-hydrolysis of A chains and external segments of B chains.
(iii) The remnants of hydrolysed longer internal chains where maltotetraosyl units have been removed.

(ii) and (iii) Become remnant external segments (or parts of A chains). These branched maltodextrins are formed extensively from the clusters of the original amylopectin.

They have a number of characteristic features. Structures with the same number of neighbouring, non-hydrolysable internal chains, but different configurations (Fig. 3) have certain similar structural properties regardless of their configuration. They have the same number of chains and of remnant external segments. Table 5 shows the values of these structural properties for maltodextrins with similar numbers of contiguous unhydrolysable chains (up to 20) as well as the general case. Several features are:

(a) The number of whole chains is equal to the number of unhydrolysed internal chains plus two ($n + 2$). This number is also equal to the number of segments plus one, with the total divided by two.
(b) The number of branch points (and branches) equals the number of internal unhydrolysable chains plus one ($n + 1$).
(c) The numbers of remnant external segments – both shortened (and any unreacted) A, remnant external B segments and remnants from hydrolysis of longer internal chains – equals the number of internal chains plus three ($n + 3$).
(d) The total number of segments equals the number of remnant external segments plus the number of unhydrolysable internal chains ($2n + 3$).

Various molecular characteristics of maltodextrins in hydrolysates can be estimated.

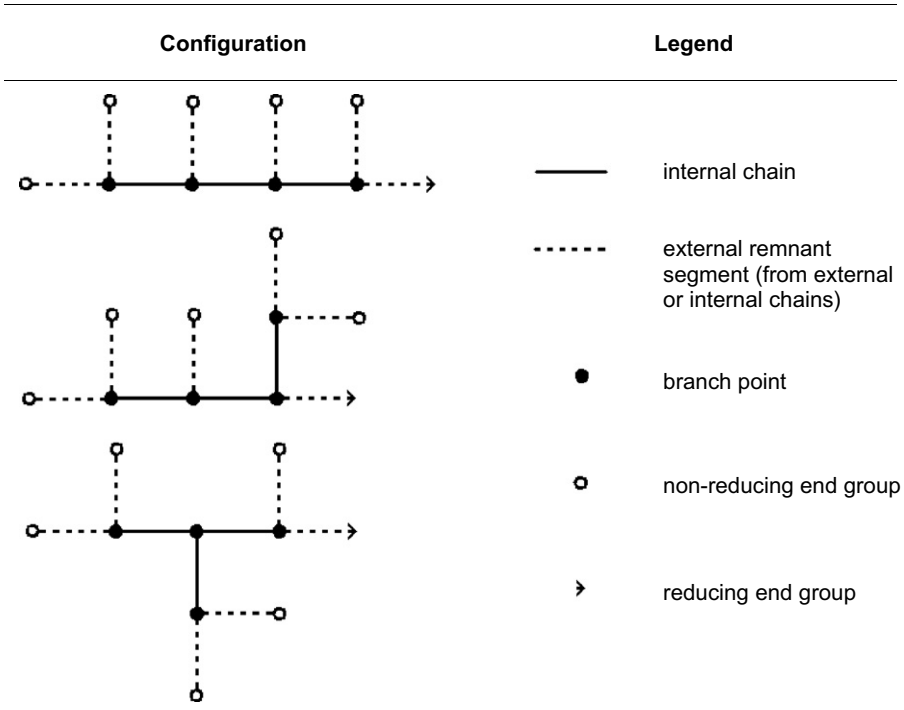

Fig. 3. Possible configurations of maltodextrins composed of five chains showing they have the same number of unhydrolysable internal chains (3), external segments (from external or internal chains) (6), branch points (4) and non-reducing end groups (5).

Table 5
Properties of maltodextrins produced by *P. stutzeri* amylase hydrolysis of the *w*-maize amylopectin model prepared from the 3D(R) construct ($E_A = 0.60$, $E_B = 0.40$, $B_A = 2$, $B_B = 2$, X, $Y = 60$, $Z = 3$, $T = 1000$, 25 replicates)

No. of unhydrolysable internal chains (n)	No. of chains ($n+2$)	No. of branch points ($n+1$)	No. of remnant segments ($n+3$)	d.p.	Average chain length[a]
0	2	1	3	15	7.3
1	3	2	4	24	8.1
2	4	3	5	34	8.6
3	5	4	6	44	8.8
5	7	6	8	64	9.1
8	10	9	11	94	9.4
18	20	19	21	193	9.6

[a] For the *w*-maize amylopectin described in Tables 2 and 3.

The weighted mean chain length (in glucosyl units) of remnant external segments in branched maltodextrin products-from both external and internal chains – is equal to

$$\frac{1}{(T+2n)}\left(\sum_{i=1}^{T}\mathrm{GE}_i+\sum_{j=1}^{n}\mathrm{GI}_j\right)$$

where GE_i is the number of remnant glucosyl units on external chain i after that chain is externally hydrolysed, GI_j is the number of remnant glucosyl units produced when linkage j is internally hydrolysed, T is the total number of chains in the original model and n is the number of internal hydrolysable linkages within the original model.

The remnant chain length of external chains equals the number of glucosyl units present prior to hydrolysis, minus four times the number of maltotetraosyl units released on hydrolysis. For hydrolysable internal chains – taking into account the branch points – it is the number of glucosyl units prior to hydrolysis minus one, minus four times the number of maltotetraosyl units released. For models of *w*-maize amylopectin and mammalian glycogen, prepared from particular constructs, the remnant chain lengths (glucosyl units) of segments composed of different numbers of g-links are shown in Tables 4A and 4B.

For a model of a specific α(1–4)(1–6) glucan, assigned the native polysaccharide's chain lengths, and prepared from a particular construct, approximations can be made of the average d.p. of released maltodextrins with a known number of unhydrolysable internal chains, as well as an approximate estimate of the M_W.

The average d.p. of the $n+1$ released maltodextrins can be expressed as:

$$\frac{1}{n+1}\left(\sum_{i=1}^{n+1}\mathrm{BP}_i+\left(\sum_{j=1}^{N_i}\mathrm{C}_j+\sum_{k=1}^{M_i}\mathrm{D}_k\right)\right)$$

where BP_i is the number of branch points, N_i is the number of remnant external segments, and M_i is the number of

unhydrolysed internal linkages in maltodextrin i respectively. C_j is the number of glucosyl units in remnant external chain j, and D_k is the number of glucosyl units in unhydrolysed linkage k.

The average chain length (in glucosyl units) of unhydrolysed internal chains can be expressed as:

$$\frac{1}{n+1}\sum_{i=1}^{n+1}\sum_{k=1}^{M_i} D_k$$

In Table 5 estimated d.p. values of maltodextrins from 2 to 20 chains produced by hydrolysis of the *w*-maize amylopectin model in Tables 2 and 4A are listed.

The average M_W of a branched maltodextrin for a specific α(1–4)(1–6) glucan derived from a particular construct can be estimated as:

The number of unhydrolysed internal chains *times* their average chain length (glucosyl units) *times* 162 *plus*.

The number, less one, of glucosyl units in remnant external segments *times* their average chain length, less one, *times* 162 *plus*.

The number of branch points *times* 145 *plus*.

The number of remnant external and internal segments *times* 179.

The end groups of internal remnant segments with a reducing end should be multiplied by 163. However, these form a small proportion of remnant chains.

Models prepared from constructs in which the g-links were assigned the lengths in glucosyl units calculated from the $n * \mathrm{ECL}/L_E$ values (for external chains) and $n * \mathrm{CCL}/L_{CC}$ (for internal chains) were subjected to simulated *P. stutzeri* hydrolysis. When the model with the chain lengths of *w*-maize amylopectin, prepared from the 3D(R) construct ($E_A = 0.40$, $E_B = 0.60$, $B_A = 2$, $B_B = 2$, X, $Y = 60$, $Z = 3$, $T = 1000$, 25 replicates, g-link total 2964, $a = 0.55$) underwent simulated hydrolysis (under the rules described in Table 4A) the extent of maltotetraose production from external and internal chains and the numbers of maltodextrins released is shown in Table 6.

The total of maltotetraose units released (2015 per 1000 chains of CL 18) was 45% of the molecule. On hydrolysis of *n*-wheat amylopectin Finch and Sebesta (1992), after SEC, obtained material with a M_W greater than that of maltotetraose of 54%. After two cycles of hydrolysis the supernatant, on ethanol precipitation, contained 57% of the original carbohydrate. In Fig. 5 the percentages of maltotetraose and the various maltodextrins obtained by this simulated hydrolysis vs their log M_W is plotted. The distribution of maltodextrins is quite different to that produced experimentally (Fig. 1 in Finch & Sebesta, 1992).They obtained a broad peak on SEC with a maximum at an elution volume similar to a fraction of dextran of M_W 15,000. After two cycles of hydrolysis and ethanol precipitation the maximum of the single peak was similar to a dextran of M_W 12,000. The chromatographic behaviour of an α-(1–4)(1–6)dextrin would be expected to be somewhat different to an α(1–6) dextran (Tao & Matheson, 1993). NMR of this maltodextrin from two hydrolysis cycles indicated a product with a d.p. of 88 (M_W 14,000) and a CL of 7.

Simulated hydrolysis of the model of *w*-maize amylopectin gave a series of maltodextrins with a maximum amount at a M_W of 2400 and then an exponential decrease as the M_W increased, so that at a M_W of 14,000 (log value 4.15, Fig. 4) only a small amount was present. An estimated 10% had a M_W above 20,000. Although the model derived from the randomly constructed 3D(R) program has a distribution of A, B and core chains similar to the native amylopectin, the distribution of internal chains is very different to the pattern found from *P. stutzeri* amylase hydrolysis of *n*-wheat amylopectin. In the 3D(R) model the major fraction of maltodextrin (both in number and amount) results from hydrolysis of a branch point linked to an A chain, an external B chain and an internal chain long enough to be hydrolysed; an external B chain and two internal chains long enough to be hydrolysed; or three internal chains long

Table 6
Products released from simulated hydrolysis by *P. stutzeri* amylase hydrolysis of a model of *w*-maize amylopectin derived from the 3D(R) construct ($E_A = 0.60$, $E_B = 0.40$, $B_A = 2$, $B_B = 2$, X, $Y = 60$, $Z = 3$, $T = 1000$, 25 replicates)

From external chains (ECL) (glucosyl units)	Number	From internal chains (ICL) (glucosyl units)	Number
Maltotetraosyl units released			
7	341	4	0
14	1247	10	162
21	113	15	64
28	37	21	24
36	8	26	11
43	2	31	2
50	1	37	1
57	1	42	1
Σ	1750	**Σ**	265

Maltodextrins released

Number of chains	2	3	4	5	6	7	8	9	10	11	12	13	14	15	16	17	18	19	20	>20
Number released	71	38	21	15	11	8	5	6	4	3	2	2	2	2	2	1	1	1	1	8

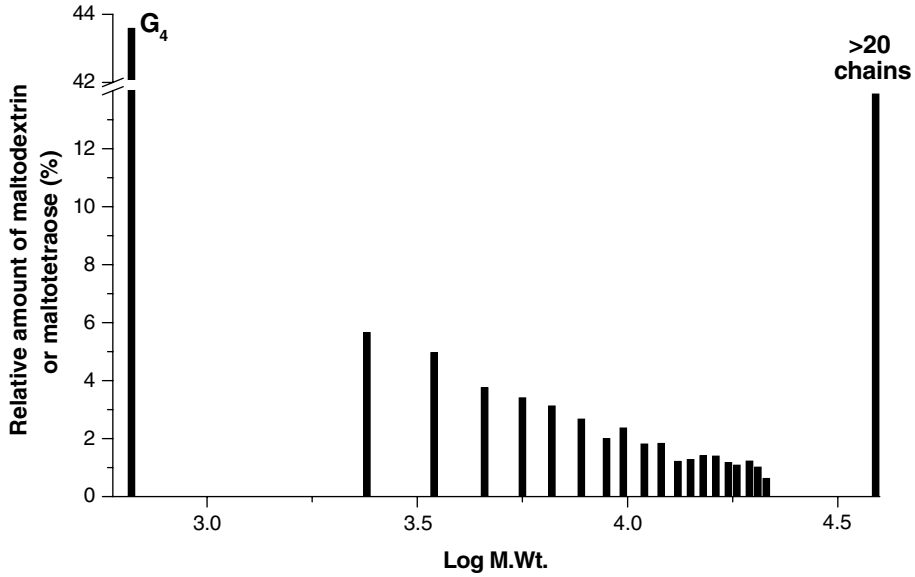

Fig. 4. Amounts of maltotetraose (G_4) and maltodextrins released on simulated hydrolysis by *P. stutzeri* amylase from a randomly constructed model of *w*-maize amylopectin.

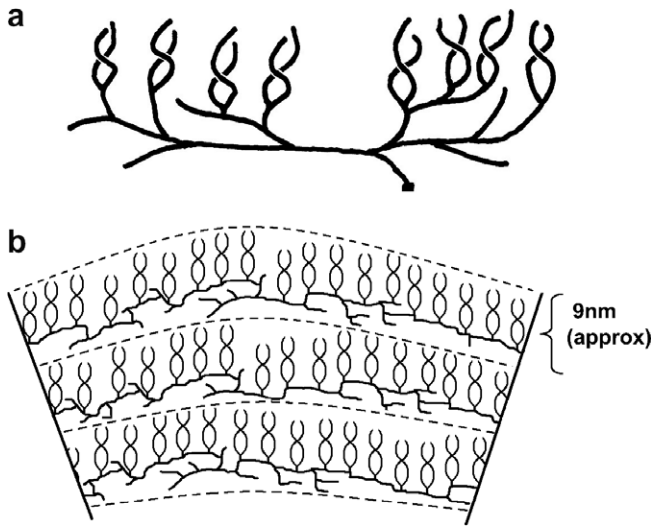

Fig. 5. (a) A schematic representation of a section across the short axis of a model with restricted extension into the third dimension. (b) A diagrammatic representation of a section of a granule across a long axis of the wafer-like polymer molecules.

enough to be hydrolysed. There are decreasing amounts of maltodextrins containing increasing numbers of short, contiguous, unhydrolysable internal chains. This pattern of maltodextrins released in the model indicates a random distribution of internal chains of different lengths. In contrast, in *n*-wheat amylopectin, the major maltodextrin fraction is distributed around a branched structure with 12–13 chains and 10–11 contiguous, unhydrolysable internal chains.

These appear to result from hydrolysis between clusters with this average structure of neighbouring, short internal chains, which are joined by longer hydrolysable internal chains. The high level of maltodextrins made up of two chains in the model of *w*-maize amylopectin – relative to those of about 10–12 chains – is in contrast to *n*-wheat amylopectin. It indicates that in the latter there are fewer branch points surrounded by external chains and one or two long internal chains, or by three long internal chains.

When other constructs were made with $E_A + E_B = 1$ (to give $a = 0.53$–0.56) with B_A and B_B ranging from 0.5 to 5 and X and Y 60 and Z 60, 3 or 0, simulated depolymerisation of the derived models gave similar patterns of decreasing amounts of maltodextrin fractions of increasing M_W.

The lower values of $(CCL + 1)/L_{CC}$ and ECL/L_E of mammalian glycogen (Tables 3 and 4B) gave a much lower extent of hydrolysis on simulated hydrolysis of its model.

The diurnal rhythm of photosynthesis gives a twofold, alternating rate of starch synthesis. More ADP–glucose – the substrate for chain elongation – is available during illumination. This suggests a possible process for the formation of clusters with short neighbouring internal chains in amylopectin. Light periods – when ADP–glucose is abundant – would provide a period of predominant chain lengthening leading to the favouring of extension over branching and hence longer internal chains. This would be followed by a period when ADP–glucose availability decreases and branching becomes the major reaction. As soon as a chain reached the minimum length for branching it would occur and lead to the formation of short internal chains. This pattern would indicate two different types of sections in the core of an amylopectin – one of longer internal chains hydrolysed by *P. stutzeri* amylase, and another of highly branched maltodextrins with contiguous, short internal chains, not hydrolysed by this amylase. It suggests a possible method of formation of a construct leading to an approximate model that involves two alternating periods; one in which the probability of extension by random addition is high relative to branching and a second in which the overriding probability of reaction is branching. This would

occur as soon as chains reached the shortest permissible length to react, leading to the highly branched sections with short internal chains. In the formation of a construct with a equal to 0.55, the average length of B chain segments (L_{BS}) increases approximately fourfold when the probability of extension relative to branching increases from 1:10 to 1:0.1 (Fig. 15 in Matheson & Caldwell, 1999).

3.4. A proposal for the arrangement of amylopectin molecules in the starch granule

Physico-chemical evidence for solubilised amylopectin indicates that it has an oblate discoid shape – a "two dimensional entity" (Banks, Geddes, Greenwood, & Jones, 1972; Callaghan & Lelievre, 1985, 1986; Callaghan, Lelievre, & Lewis, 1987; Durani & Donald, 2000; Kerr, 1945). Ultracentrifugation in DMSO demonstrated that wheat amylopectin was a highly planar molecule with semi-axes of 45 and 1.2 nm (Lelievre, Lewis, & Marsden, 1986). Its β-limit dextrin was still a flat disc. In aqueous solution the individual molecules appear to associate. A flat discoidal shape for amylopectin is in accord with the large decrease in viscosity and increase in elution volume on SEC of the derived β-limit dextrin, after periodate oxidation and borohydride reduction, when the acyclic structure of the opened α(1–4) pyranose rings allows the formation of a more compact globular shape (Tao & Matheson, 1993). In contrast, the β-limit dextrin of mammalian glycogen – it already has a globular shape, since on ultracentrifugation S_0 has only a slight dependence on concentration (Banks et al., 1972) – shows little change in elution volume relative to the M_W change when it is oxidised and reduced.

It has been shown that if a construct is made with limited extension along one axis, simulated debranching of a model made from this with the various chain length values of *w*-maize amylopectin gives a chromatographic pattern similar to that found experimentally for the native amylopectin (Caldwell & Matheson, 2003). Also, debranched β-limit dextrin of *w*-maize amylopectin gives a similar profile on reaction to simulated hydrolysis of a model (Section 3.1). From this information and the degree of crystallinity observed in amylopectin in the solid state (Cooke & Gidley, 1992; Imberty et al., 1991; Gidley & Bociek, 1985; Jenkins et al., 1993) a model can be proposed in which the macromolecule has a wafer-like form and the biosynthetic reactions of chain extension and branching occur essentially in a plane of two axes with limited extension into the third axis. Then double-helical structures formed between the outermost segments of B chains (external B chains) and A chains that are outermost chains attached to these B segments adopt a conformation with the axes of their double-helices perpendicular to the two major dimensions. In a two-dimensional construct (Fig. 3 in Caldwell & Matheson, 2003) in which the outermost segments of B chains have A chains attached as their outermost chains – and so capable of forming parallel double-helical structures – they are found spread over the surface of the two-dimensional plane, providing the material for the crystalline region. Almost 40% lie close to or within the radius of gyration. The large decrease in the a value of *w*-maize amylopectin, partly debranched by pullulanase, (Manners & Matheson, 1981) is in agreement with this interpretation. A section across the short axis of a model with restricted extension into the third dimension is shown in Fig. 5a. It consists of two parts, an irregular, amorphous zone composed of B chains (mostly interior to outermost B segments) as well as A chains that are not outermost A chains; and a crystalline region composed of parallel double-helices made up of outermost B segments and A chains that are linked as outermost branches to these.

The growth of starch granules occurs by sequential layering onto the outer surface of the granule – apposition (Badenhuizen & Dutton, 1956; Buttrose, 1962). In the 3D(R) construct synthesis of newly forming polymer molecules, by growth of chains along the long axes (X and Y) can occur in both positive and negative directions ($\pm X$ and $\pm Y$) and is essentially not limited in these directions. Along the short (Z) axis growth is only possible in one direction ($+Z$ or not at all if $Z = 0$), that is, outwards from the centre of the granule – and it is limited to a short distance. Production of the combination of an outermost B chain with an A chain attached as an outermost branch can occur at the termination of growth of a B chain. Limited growth of chains along the Z axis, combined with non-limited development of chains in the X–Y plane would then lead to a wafer-like form. The outer layer consists of a region of double-helical chains derived from outermost B segments with an A chain attached as the outermost branch, plus an inner zone of B chains with other B chains attached as outermost chains, and with A chains occurring as branches at all positions except as outermost chains. The chains in the inner zone would be incapable of forming parallel double-helical structures. Since re-precipitation of solubilised starch gives a product with a crystalline fraction (Gidley & Bociek, 1985) it appears that the formation of the parallel double-helical structure from outermost B segments and outermost A chains attached to them is a spontaneous process. The lack of crystallinity in glycogen and phytoglycogen may be due the insufficient length of their A and external B chains to form double-helical structures.

The individual polymer molecules are layered with their long axes (X and Y) perpendicular to the radial axis of the granule. Fig. 5b shows a diagrammatic representation of a section of a granule across a long axis of the wafer-like polymer molecules. In the crystalline region the long axes of the parallel double-helices are directed radially. The amorphous zone in each wafer-like structure lies towards the centre of the granule: that is, it is the inner layer of each molecule. This concentric layering of the polymer molecule gives a repeating pattern, which has been detected by small angle X-ray scattering for the granules of six starch species (Jenkins et al., 1993). For an amylopectin in which the average length of A chains is 12 glucosyl units and the h value .35 nm, the width of parallel double-helical region

would be 4.2 nm. Then a repeat distance of 9 nm (from small angle X-ray scattering) would indicate a thickness of the amorphous zone of 4.8 nm.

Nageli dextrins arise from the relative resistance to acidic hydrolysis – compared to unpaired linkages in the amorphous zone – of the double-helical structures in the crystalline region. Association by double helix formation between neighbouring polymer molecules (both laterally and radially) may occur via amylose chains and longer than average external amylopectin chains: in this case parallel and anti-parallel alignment may both be possible.

The reaction of the amylase from *P. stutzeri* with parallel double-helical structures formed from outermost B segments and an outermost attached A chain would produce a branched α(1–4)(1–6) dextrin composed of two α(1–4) chains, provided the internal B chain linking to the main chain was long enough. If this linking internal chain is too short for hydrolysis it will become part of a dextrin of more than two chains, with the remainder derived from the amorphous zone. Dextrins composed of two α(1–4) chains can also be produced from the amorphous zone where a 1,4,6 linked glucosyl unit is linked to three long internal chains. The branched α(1–4) dextrins of more than two chains consist of internal chains too short to be hydrolysed by the amylase. Although *P.stutzeri* amylase hydrolysis of wheat amylopectin produced dextrins with a range of M_W values, the peak at a single value of near to 14,000 was consistent with a cluster structure (Finch & Sebesta, 1992).

References

Andrews, P. (1965). The gel-filtration behaviour of proteins related to their molecular weights over a wide range. *Biochemical Journal, 96*, 595–606.

Baba, T., & Arai, Y. (1984). Structural characterization of amylopectin and intermediate material in amylomaize starch granules. *Agricultural and Biological Chemistry, 48*, 1763–1775.

Badenhuizen, N. P., & Dutton, R. W. (1956). Growth of ^{14}C-labelled starch granules in potato tubers as revealed by autoradiographs. *Protoplasma, 47*, 156–163.

Banks, W., Geddes, R., Greenwood, C. T., & Jones, I. G. (1972). The molecular size and shape of amylopectin. *Starch, 24*, 245–251.

Bertoft, E. (2004). On the nature of categories of chains in amylopectin and their connection to the super helix model. *Carbohydrate Polymers, 57*, 211–224.

Bertoft, E., & Spoof, L. (1989). Fractional precipitation of amylopectin alpha-dextrins using methanol. *Carbohydrate Research, 189*, 169–180.

Bertoft, E., Zhu, Q., Andtfolk, H., & Jungner, M. (1999). Structural heterogeneity in waxy-rice starch. *Carbohydrate Polymers, 38*, 349–359.

Bertoft, E., & Koch, K. (2000). Composition of chains in waxy-rice starch and its structural units. *Carbohydrate Polymers, 41*, 121–132.

Buttrose, M. S. (1962). The influence of environment on the shell structure of starch granules. *Journal of Cell Biology, 14*, 159–167.

Caldwell, R. A., & Matheson, N. K. (2003). a-(1–4) Chain distributions of three-dimensional, randomly generated model, amylopectin and mammalian glycogen: Comparisons of chromatograms of debranched chains of these polysaccharides and models with random dendrimeric models with the same chain lengths (CL, ICL, ECL) and fractions of A chains. *Carbohydrate Polymers, 54*, 201–213.

Callaghan, P. T., & Lelievre, J. (1985). The size and shape of amylopectin: A study using pulsed-field gradient nuclear magnetic resonance. *Biopolymers, 24*, 441–460.

Callaghan, P. T., & Lelievre, J. (1986). The influence of polymer size and shape on self-diffusion of polysaccharides and solvents. *Analytica Chimica Acta, 189*, 145–166.

Callaghan, P. T., Lelievre, J., & Lewis, J. A. (1987). A comparison of the size and shape of b-limit dextrin and amylopectin using pulsed field-gradient nuclear magnetic resonance and analytical ultracentrifugation. *Carbohydrate Research, 162*, 33–40.

Cooke, D., & Gidley, M. J. (1992). Loss of crystalline and molecular order during starch gelatinization: Origin of the enthalpic transition. *Carbohydrate Research, 227*, 103–112.

Durani, C. M., & Donald, A. M. (2000). Shape, molecular weight distribution and viscosity of amylopectin in dilute solution. *Carbohydrate Polymers, 41*, 207–217.

Enevoldson, B. S., & Juliano, B. O. (1988). Ratio of A to B chains in rice amylopectins. *Cereal Chemistry, 65*, 424–427.

Finch, P., & Sebesta, D. W. (1992). The amylase of *Pseudomonas stutzeri* as a probe of the structure of amylopectin. *Carbohydrate Research, 227*, C1–C4.

French, D. (1984). Organisation of starch granules. In R. L. Whistler, J. N. Be Miller, & J. F. Paschall (Eds.), *Starch: Chemistry and technology* (pp. 183–247). Orlando: Academic Press.

Gallant, D. J., Bouchet, B., & Baldwin, P. M. (1997). Microscopy of starch: Evidence of a new level of granule organization. *Carbohydrate Polymers, 32*, 177–191.

Gidley, M. J., & Bociek, S. M. (1985). Molecular organization in starches. A ^{13}C CP/ MAS NMR study. *Journal American Chemical Society, 107*, 7040–7044.

Hizukuri, S. (1986). Polymodal distribution of chain lengths of amylopectins, and its significance. *Carbohydrate Research, 147*, 342–347.

Imberty, A., Buleon, A., Tran, V., & Perez, S. (1991). Recent advances in the knowledge of starch structure. *Starch, 43*, 375–384.

Inouchi, N., Glover, D. V., & Fuwa, H. (1987). Chain length distribution of amylopectins of several single mutants and the normal counterpart, and sugary-1 phytoglycogen in maize (Zea mays L). *Starch, 39*, 259–266.

Jane, J., Chen, Y., Lee, L. F., M^{c}Pherson, A. E., Wong, K. S., Radosavljevic, M., & Kasemsuwan, T. (1999). Effects of amylopectin branch chain length and amylose content on the pasting properties of starch. *Cereal Chemistry, 76*, 629–637.

Jenkins, P. J., Cameron, R. E., & Donald, A. M. (1993). A universal feature in the structure of starch granules from different botanical sources. *Starch, 45*, 417–420.

Kainuma, K. (1988). Structure and chemistry of the starch granule. In P. K. Stumpf & E. E. Conn (Eds.), *Biochemistry of plants. Carbohydrates* (Vol. 14, pp. 144–180). J. Preiss.

Kerr, R. W. (1945). The heterogeneity of amylose and amylopectin, part 1. *Archives of Biochemistry, 7*, 377–392.

Klucinec, J. D., & Thompson, D. B. (2002). Structure of amylopectins from ae-containing maize starches. *Cereal Chemistry, 79*, 19–23.

Lelievre, J., Lewis, J. A., & Marsden, K. (1986). The size and shape of amylopectin. A study using analytical ultracentrifugation. *Carbohydrate Research, 153*, 195–203.

MacGregor, A. W., & Morgan, J. E. (1984). Structure of amylopectins isolated from large and small starch granules of normal and waxy barley. *Cereal Chemistry, 61*, 222–228.

Manners, D. J. (1989). Recent developments in our understanding of amylopectin structure. *Carbohydrate Polymers, 11*, 87–112.

Manners, D. J., & Matheson, N. K. (1981). The fine structure of amylopectin. *Carbohydrate Research, 90*, 99–110.

Matheson, N. K. (1995). The chemical structure of amylase and amylopectin fractions of starch from tobacco leaves during development and diurnally-nocturnally. *Carbohydrate Research, 282*, 247–262.

Matheson, N. K., & Caldwell, R. A. (1999). a(1–4) Chain disposition in models of a(1–4)glucans: Comparison with structural data for mam-

malian glycogen and waxy amylopectin. *Carbohydrate Polymers, 40*, 191–209.

Mercier, C. (1973). The fine structure of corn starches of various amylase percentages; waxy, normal and amylomaize. *Starch, 25*, 78–83.

Nakakuki, T., Azuma, K., & Kainuma, K. (1984). Action patterns of various exo-amyloses and the anomeric configurations of their products. *Carbohydrate Research, 128*, 297–310.

Nikuni, Z. (1978). Studies on starch granules. *Starch, 30*, 105–111.

Oostergetel, G. T., & van Bruggen, E. F. J. (1993). The crystalline domains in potato starch granules are arranged in a helical fashion. *Carbohydrate Polymers, 21*, 7–12.

Priest, F. G., Goodfellow, M., Shute, L. A., & Berkeley, R. C. W. (1987). Bacillus amyloliquefaciens sp. nov., nom. rev. *International Journal of Systematic Bacteriology, 37*, 69–71.

Robin, J. P., Mercier, C., Duprat, F., Charbonniere, R., & Guilbot, A. (1975). Etudes chromatographic et enzymatique des residues insolubles provenant de l'hydrolyse chlorhydrique d'amidons de cereales, en particular de mais cireux. *Starch, 27*, 36–45.

Robyt, J. F., & Ackerman, R. J. (1971). Isolation, purification and characterization of a maltotetraose producing amylase from *Pseudomonas stutzeri. Archives of Biochemistry and Biophysics, 145*, 105–114.

Robyt, I., & French, D. (1963). Action pattern and specificity of an amylase from *Bacillus subtilis. Archives of Biochemistry and Biophysics, 100*, 451–467.

Schmidt, J., & John, M. (1979). Starch metabolism in Pseudomonas stutzeri. 1. Studies on maltotetraose- forming amylase. *Biochimica Biophysica Acta, 566*, 88–99.

Shi, Y-C., & Seib, P. A. (1995). Fine structure of maize starches from four wx-containing genotypes of the W64A inbred line in relation to gelatinization and retrogradation. *Carbohydrate Polymers, 26*, 141–147.

Tao, L., & Matheson, N. K. (1993). The role of structure on the molecular size and conformation of (1–4) and (1–6) linked polysaccharides. *Carbohydrate Polymers, 20*, 269–277.

Waigh, T. A., Kato, K. L., Donald, A. M., Gidley, M. J., Clarke, C. J., & Riekel, C. (2000). Side-chain liquid-crystalline model for starch. *Starch, 52*, 450–460.

Wong, K. S., & Jane, J. (1997). Quantitative analysis of debranched amylopectin by HPAEC-PAD with a postcolumn enzyme reactor. *Journal of Liquid Chromatography and Related Technology, 20*, 297–310.

Yamaguchi, M., Kainuma, K., & French, D. (1979). Electron microscope observation of waxy maize starch. *Journal of Ultrastructure Research, 69*, 249–261.

Yuan, R. C., Thompson, D. B., & Boyer, C. D. (1993). Fine structure of amylopectin in relation to gelatinization and retrogradation behaviour of maize starches from three wx-containing genotypes in two inbred lines. *Cereal Chemistry, 70*, 81–89.

Yun, S-H., & Matheson, N. K. (1993). Structures of the amylopectins of waxy, normal, amylase-extender and wx:ae genoyypes and the phytoglycogen of maize. *Carbohydrate Research, 243*, 307–321.

Zobel, H. F. (1988). Molecules to granules: a comprehensive starch review. *Starch, 40*, 44–50.